

Article

# The Magnetic Properties of 1111-type Diluted Magnetic Semiconductor $(\text{La}_{1-x}\text{Ba}_x)(\text{Zn}_{1-x}\text{Mn}_x)\text{AsO}$ in the Low Doping Regime

Guoxiang Zhi <sup>1</sup>, Kai Wang <sup>1</sup>, Haojie Zhang <sup>1</sup>, Cui Ding <sup>1</sup>, Shengli Guo <sup>1</sup>, Yilun Gu <sup>1</sup>, Licheng Fu <sup>1</sup> and F. L. Ning <sup>1,2,\*</sup>

<sup>1</sup> Department of Physics, Zhejiang University, Hangzhou 310027, China; nucbill@zju.edu.cn (G.Z.); Kudoukai@zju.edu.cn (K.W.); havoc@zju.edu.cn (H.Z.); dingcui@zju.edu.cn (C.D.); slguo@zju.edu.cn (S.G.); 11636019@zju.edu.cn (Y.G.); 3120103824@zju.edu.cn (L.F.)

<sup>2</sup> Collaborative Innovation Center of Advanced Microstructures, Nanjing University, Nanjing 210093, China

\* Correspondence: ningfl@zju.edu.cn

Received: 14 September 2018; Accepted: 26 November 2018; Published: date



**Abstract:** We investigated the magnetic properties of  $(\text{La}_{1-x}\text{Ba}_x)(\text{Zn}_{1-x}\text{Mn}_x)\text{AsO}$  with  $x$  varying from 0.005 to 0.05 at an external magnetic field of 1000 Oe. For doping levels of  $x \leq 0.01$ , the system remains paramagnetic down to the lowest measurable temperature of 2 K. Only when the doping level increases to  $x = 0.02$  does the ferromagnetic ordering appear. Our analysis indicates that antiferromagnetic exchange interactions dominate for  $x \leq 0.01$ , as shown by the negative Weiss temperature fitted from the magnetization data. The Weiss temperature becomes positive, i.e., ferromagnetic coupling starts to dominate, for  $x \geq 0.02$ . The Mn–Mn spin interaction parameter  $|2J/k_B|$  is estimated to be in the order of 10 K for both  $x \leq 0.01$  (antiferromagnetic ordered state) and  $x \geq 0.02$  (ferromagnetic ordered state). Our results unequivocally demonstrate the competition between ferromagnetic and antiferromagnetic exchange interactions in carrier-mediated ferromagnetic systems.

**Keywords:** ferromagnetic ordering; antiferromagnetic exchange interaction; ferromagnetic coupling; carrier-mediated

## 1. Introduction

Combining the properties of semiconductor and magnetism, diluted magnetic semiconductors (DMSs) have potential application in industry [1–3]. In the 1980s, the focus was mainly on II–VI DMSs  $\text{A}_{1-x}^{\text{II}}\text{Mn}_x\text{B}^{\text{VI}}$  ( $\text{A} = \text{Zn, Cd, Hg}$ ;  $\text{B} = \text{Se, Te}$ ), where iso-valent substitution of  $\text{Mn}^{2+}$  for  $\text{A}^{2+}$  in  $\text{A}^{\text{II}}\text{B}^{\text{VI}}$  usually induces spin glass [1]. The research of DMSs has become explosive since III–V DMSs (In,Mn)As and (Ga,Mn)As were successfully fabricated via low temperature molecular beam epitaxy in the 1990s [2–9]. It was initially proposed that the Curie temperature  $T_C$  of III–V DMSs would reach room temperature assuming sufficient Mn ions could be doped homogeneously [10]. However, after more than two decades of effort, the highest  $T_C$  of  $(\text{Ga}_{1-x}\text{Mn}_x)\text{As}$  has been reported as  $\sim 200$  K with  $x \sim 12\%$  [11–13]. Some difficulties are encountered in the research of (Ga,Mn)As. Firstly, it is difficult to increase Mn concentration while keeping thin films homogeneous due to the low solid solubility of Mn in GaAs. Secondly, Mn substitution for GaAs provides not only local moments but also carriers. Moreover, some  $\text{Mn}^{2+}$  ions behave as double donors when getting into interstitial sites [3]. Thirdly, it seems that  $T_C$  does not increase above 200 K where even higher Mn doping levels could be achieved, i.e.,  $T_C$  saturates at  $\sim 200$  K. The possible reason is that  $\text{Mn}^{2+}$  are more likely to have another  $\text{Mn}^{2+}$  at nearest-neighbour sites for higher Mn doping levels, which results in antiferromagnetic exchange interactions that compete with the ferromagnetic ordering.

Recently, several bulk form DMS systems derived from Fe-based superconductors have been reported [13–26]. Similar to the style used in Fe-based superconductors, these DMS systems are named as “111” [14–17], “122” [18–20], “1111” [21–26], and “32522” [27] type DMSs. The progress on this research stream can be found in a recent review article [28]. The bulk form DMSs have some advantages. Firstly, we can apply conventional magnetic probes, such as muon spin relaxation ( $\mu$ SR) and nuclear magnetic resonance (NMR) to investigate the ferromagnetism at a microscopic level.  $\mu$ SR measurements have confirmed that the ferromagnetism in these DMSs is homogeneous and shares the same mechanism as that of (Ga,Mn)As [14,17,18,21,24,29]. On the other hand, NMR results of Li(Zn<sub>0.9</sub>Mn<sub>0.1</sub>)P have demonstrated that Mn–Mn spin interactions are mediated by hole carriers, and the averaged ferromagnetic exchange interactions are in the order of 100 K [30]. Another advantage of these bulk form DMSs is that we can control the doping concentrations of spins and carriers separately, and their individual influence on ferromagnetic ordering can be investigated. For example, we found that there is no ferromagnetic order occurring when only doping Mn into the parent compound LaZnAsO up to 10% [21]. The ferromagnetic order does not develop until carriers and spins are codoped into LaZnAsO. On the other hand, for a fixed amount of Mn concentration, too many carriers will suppress Curie temperature instead [17,22].

From theoretical point of view, the NMR results on Li(Zn<sub>0.9</sub>Mn<sub>0.1</sub>)P are consistent with the theoretical model that spin interactions are mediated by conduction carriers to form long range magnetic order. The long range ferromagnetic order has been explained by the p-d Zener exchange model [10], which is an analog of the Ruderman–Kittel–Kasuya–Yosida (RKKY) interaction in metals. However, in the very dilute regime, i.e., the concentrations of both spins and carriers are at a very low levels, carriers might be localized and cannot mediate the spin interactions. Bound magnetic polaron (BMP) model, which proposes that the percolation of magnetic polarons will induce ferromagnetic ordering, has been applied to explain the mechanism in the very dilute regime of DMSs [31].

We fully used the advantages of decoupled charge and spin doping in (La<sub>1-x</sub>Ba<sub>x</sub>)(Zn<sub>1-x</sub>Mn<sub>x</sub>)AsO, and investigated the magnetic properties in the very dilute doped regime. We codoped Ba and Mn into the direct gap parent semiconductor LaZnAsO at low doping concentration,  $x \leq 0.05$  (more details about the synthesis and characterizations of (La<sub>1-x</sub>Ba<sub>x</sub>)(Zn<sub>1-x</sub>Mn<sub>x</sub>)AsO with higher doping level can be found in Ref. [21]). We measured the magnetization at  $B_{ext} = 1000$  Oe and fit the data above  $T_C$  to obtain the Weiss temperature  $\theta$ . Our fitting results indicate that weak antiferromagnetic exchange coupling dominates for  $x \leq 0.01$ , and ferromagnetic coupling starts to dominate for  $x \geq 0.02$ . We calculated the Mn–Mn spin interactions parameter  $J$ , and  $2J/k_B$  is about  $-10 \text{ K} \pm 3 \text{ K}$  for  $x \leq 0.01$  and about  $17 \text{ K} \pm 5 \text{ K}$  for  $x \geq 0.02$ , which are in the same order as that of Hg<sub>1-x</sub>Mn<sub>x</sub>Te [32]. We show that the random nature of the spin interactions for the doping regime of  $x \leq 0.01$  can be explained by models based on random-exchange interactions [33–36].

## 2. Results and Discussion

In Figure 1a, we show the dc-magnetization of La(Zn<sub>0.9</sub>Mn<sub>0.1</sub>)AsO measured under field cooling (FC) and zero field cooling (ZFC) condition with  $B_{ext} = 1000$  Oe. The two curves are superposed to each other in the whole measured temperature range and can be well fitted by a Curie–Weiss relation  $M = \frac{C}{T-\theta} + M_0$ , suggesting a paramagnetic ground state, where  $M_0$  is temperature independent part induced by the host lattice (LaZnAsO).  $(M - M_0)^{-1}$  versus  $T$  (15 K to 200 K) is shown in Figure 1b. The intercept in the T-axis is the Weiss temperature,  $\theta = -2.6$  K, indicating the antiferromagnetic coupling. The negative intercept was also found for Hg<sub>1-x</sub>Mn<sub>x</sub>Te and Pb<sub>1-x</sub>Mn<sub>x</sub>Te, and other II-VI [33] and IV-VI [32] DMSs. In Figure 1c, we show the plot of  $\ln(M)$  versus  $\ln(T)$ , which can be fitted by a straight line  $\ln(M - M_0) = -1.52 - 0.68\ln(T)$ . This behavior indicates that the magnetization of La(Zn<sub>0.9</sub>Mn<sub>0.1</sub>)AsO follows a power-law dependence with temperature, with the slope  $\alpha = -0.68$ . The well fitted results are consistent with models based on random-exchange interactions [33–36]. In these models, the low-temperature magnetization in a system with random exchange interactions in any dimensions follows a power-law with temperature as  $T^\alpha$  ( $-1 \leq \alpha \leq 0$ ) [33]. The magnitude of  $\alpha$  is a

measure of how random the spin interactions are. For example,  $\alpha = -1$  corresponds to the standard Curie-law behavior [33].

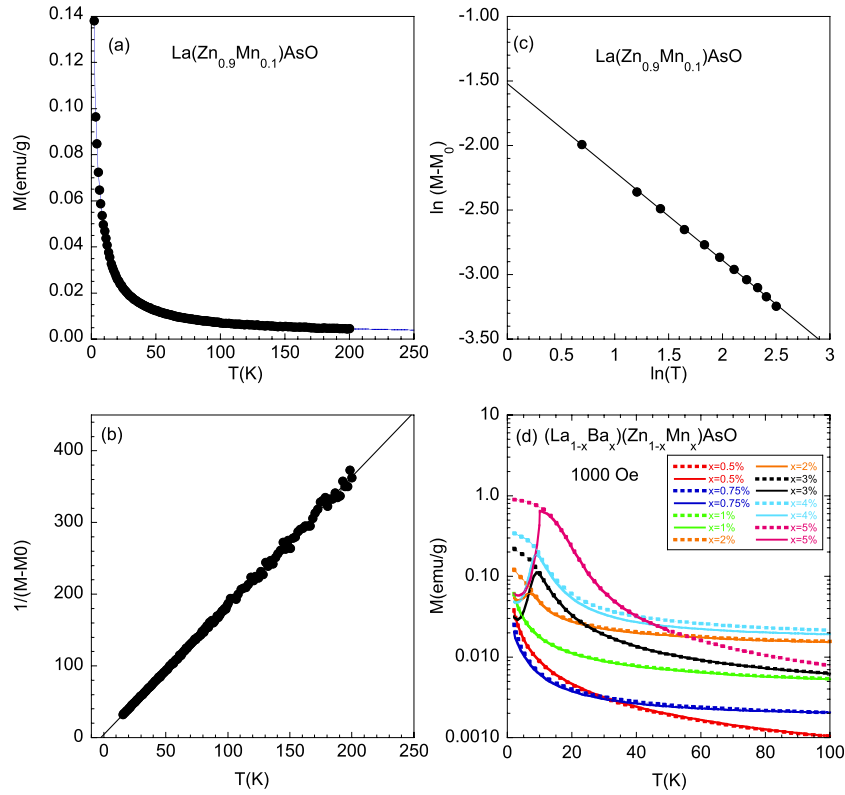


**Figure 1.** (Color online) (a) Temperature dependence of magnetization for LaZn<sub>0.9</sub>Mn<sub>0.1</sub>AsO under field cooling and zero field cooling at  $B_{ext} = 1000$  Oe; the solid line represents the Curie–Weiss fit for temperature range of 15–200 K. (b) Linear fit for  $1/(M - M_0)$  of LaZn<sub>0.9</sub>Mn<sub>0.1</sub>AsO for the temperature range of 15–200 K, where  $M_0$  is a temperature independent parameter derived from the Curie–Weiss fit. (c)  $\ln(M - M_0)$  versus  $\ln(T)$  for LaZn<sub>0.9</sub>Mn<sub>0.1</sub>AsO. (d) Temperature dependence of magnetization for  $(La_{1-x}Ba_x)(Zn_{1-x}Mn_x)AsO$  ( $x = 0.005 \sim 0.05$ ) measured under field cooling (dashed lines) and zero field cooling (solid lines) at  $B_{ext} = 1000$  Oe.

We show the field cooling (FC) and zero field cooling (ZFC) dc-magnetization of  $(La_{1-x}Ba_x)(Zn_{1-x}Mn_x)AsO$  ( $x = 0.005 \sim 0.05$ ) for  $B_{ext} = 1000$  Oe in Figure 1d. The magnitude of magnetization at low temperature (2 K) measured under FC condition increases from 0.039 emu/g ( $x = 0.005$ ) to 0.903 emu/g ( $x = 0.05$ ). For  $x \leq 0.01$ , no magnetic instability or anomaly is observed in both FC and ZFC curves, indicating there is no ferromagnetic or spin-glass ordering induced. Starting from  $x = 0.02$ , a clear splitting between FC and ZFC curves at low temperature can be observed. We fit the data of susceptibility ( $M/H$ ) at high enough (much higher than  $\theta$ ) temperature by a Curie–Weiss law  $\chi = \frac{C}{T-\theta} + \chi_0$ , where  $\chi_0$  is temperature independent part induced by the host lattice,  $C$  is the Curie constant and  $\theta$  the Weiss temperature. With the number  $C$ , we can calculate the effective occupation probability of magnetic ion on a Zn site,  $\bar{x}$ . Considering a modified Brillouin function with Weiss' molecule field theory, the magnetization of  $\bar{x}N_0$  Mn ions is  $M = S_{Mn}g_{Mn}\mu_B\bar{x}N_0B_{S_{Mn}}(\xi)$ , where  $\xi = \frac{g_{Mn}\mu_B S_{Mn} H_{eff}}{k_B T}$ ,  $H_{eff} = H_e + \lambda M$ ,  $S_{Mn}$  is the spin of Mn,  $g_{Mn}$  is the spin-splitting  $g$  factor of Mn,  $\mu_B$  is the Bohr magneton,  $N_0$  is the number of Zn site per gram,  $k_B$  is the Boltzmann constant,  $H_{eff}$  is the effective magnetic field,  $H_e$  is the applied field and  $\lambda$  is a constant. Since the Brillouin function  $B_S(\xi) = \frac{S+1}{35}\xi + O(x^3)$ , we have  $\chi = \frac{\bar{x}N_0(g_{Mn}\mu_B)^2 S_{Mn}(S_{Mn}+1)}{3k_B(T-\theta')}$ , where  $\theta' = \frac{\bar{x}N_0(g_{Mn}\mu_B)^2 S_{Mn}(S_{Mn}+1)\lambda}{3k_B}$ . Comparing with the Curie–Weiss law, we have  $\theta' = \theta$  and  $\bar{x} = \frac{3k_B C M_{mol}}{(g_{Mn}\mu_B)^2 S_{Mn}(S_{Mn}+1)N_A}$ , where  $M_{mol}$  is the

formula weight and  $N_A$  is the Avogadro number. We assume that  $g_{Mn} = 2$  and  $S_{Mn} = \frac{5}{2}$  (this assumption is reasonable because the effective moment from experiments is estimated to be  $4\text{--}5 \mu_B/\text{Mn}$  [21]).

From the Heisenberg model, if we count only the nearest-neighbor exchange interaction of Mn ions, we can derive the molecular field  $H_{mf} = \lambda M = \frac{1}{g\mu_B} \sum_{\mathbf{R}'} \bar{x} J(\mathbf{R} - \mathbf{R}') S(\mathbf{R}')$ . Assuming every spin has the same value and sums up to give the total magnetization, we have  $S(\mathbf{R}') = \frac{M}{g\mu_B \bar{x} N_0}$ , and  $\lambda = \frac{2\bar{x}zJ}{\bar{x}N_0(g\mu_B)^2}$ . Under the circumstance that temperature is in the range where no long-range magnetic order formed, the nearest-neighbor exchange interaction can be estimated by using  $\theta$  and  $\bar{x}$  from the relation  $J = \frac{3\theta k_B}{2\bar{x}S_{Mn}(S_{Mn}+1)z}$ , where  $z$  is the number of nearest neighbors on Zn site.  $z$  equals to 4 in  $(\text{La}_{1-x}\text{Ba}_x)(\text{Zn}_{1-x}\text{Mn}_x)\text{AsO}$  system.

In Table 1, we list the concentration  $x$ , obtained  $\bar{x}$ ,  $\theta$  and  $J$  for  $(\text{La}_{1-x}\text{Ba}_x)(\text{Zn}_{1-x}\text{Mn}_x)\text{AsO}$ . The small negative Weiss temperature  $\theta$  for  $x \leq 0.01$  indicates that weak antiferromagnetic interactions dominate. On the other hand, starting from  $x = 0.02$ , the Weiss temperature  $\theta$  turns into a positive value, indicating ferromagnetic interactions start to dominate. Note that, in  $\text{Pb}_{1-x}\text{Eu}_x\text{Te}$ , the coupling between Eu ions is still antiferromagnetic for the doping level up to 31.6 % [32].

**Table 1.** Weiss temperature ( $\theta$ ) and the nearest neighbor exchange interaction for  $(\text{La}_{1-x}\text{Ba}_x)(\text{Zn}_{1-x}\text{Mn}_x)\text{AsO}$ .

| $x$    | $\bar{x}$           | $\theta$ (K)   | $2J/k_B$ (K) |
|--------|---------------------|----------------|--------------|
| 0.005  | $0.0064 \pm 0.0003$ | $-0.9 \pm 0.1$ | -11.71       |
| 0.0075 | $0.0034 \pm 0.0002$ | $-0.3 \pm 0.1$ | -7.47        |
| 0.01   | $0.011 \pm 0.001$   | $-1.7 \pm 0.2$ | -13.45       |
| 0.02   | $0.018 \pm 0.001$   | $2.5 \pm 0.2$  | 12.12        |
| 0.03   | $0.032 \pm 0.002$   | $5.8 \pm 0.1$  | 15.44        |
| 0.04   | $0.046 \pm 0.003$   | $6.2 \pm 0.1$  | 11.64        |
| 0.05   | $0.066 \pm 0.003$   | $16.2 \pm 0.2$ | 21.22        |

In the first approximation,  $\frac{\theta}{S_{Mn}(S_{Mn}+1)z}$  should depend linearly on  $\bar{x}$  and go to zero when  $\bar{x}$  goes to zero, with a slope of  $\frac{2J}{3k_B}$  [32]. We show the plot of  $\frac{\theta}{S_{Mn}(S_{Mn}+1)z}$  versus  $\bar{x}$  of  $(\text{La}_{1-x}\text{Ba}_x)(\text{Zn}_{1-x}\text{Mn}_x)\text{AsO}$  for  $0.005 \leq x \leq 0.01$  and  $0.02 \leq x \leq 0.05$  in Figure 2a,b, respectively. The dashed linear lines passing through the origin are guides for eyes. In Figure 2, the data points are not far away from a linear line, which gives evidence for the validity of calculating  $\bar{x}$  with such method.

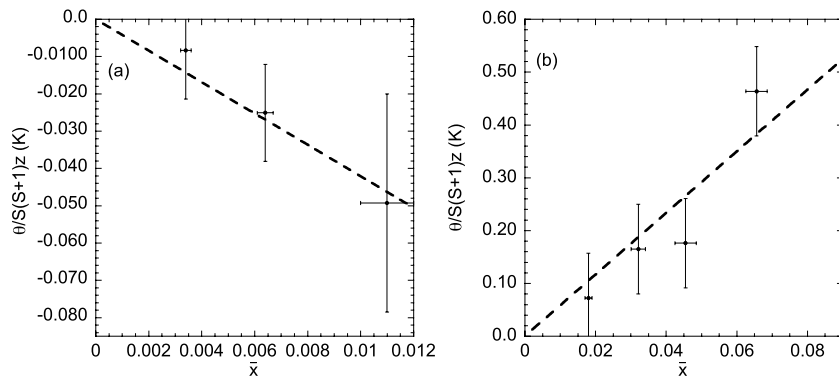


**Figure 2.** The parameter  $\frac{\theta}{S_{Mn}(S_{Mn}+1)z}$  versus the effective magnetic ion concentration  $\bar{x}$  in  $(\text{La}_{1-x}\text{Ba}_x)(\text{Zn}_{1-x}\text{Mn}_x)\text{AsO}$  for: (a)  $0.005 \leq x \leq 0.01$ ; and (b)  $0.02 \leq x \leq 0.05$ . Dashed lines are guides for eyes.

For  $x \geq 0.02$ , the nearest-neighbor interaction parameter  $|2J/k_B|$  of  $(\text{La}_{1-x}\text{Ba}_x)(\text{Zn}_{1-x}\text{Mn}_x)\text{AsO}$  with ferromagnetic coupling is about  $17 \text{ K} \pm 5 \text{ K}$ . For  $x \leq 0.01$ , with antiferromagnetic coupling,  $|2J/k_B|$  is about  $10 \text{ K} \pm 3 \text{ K}$ , which is in the same order of magnitude as that in Mn-doped II-VI systems [32]. For instance,  $|2J/k_B|$  for Mn-doped HgSe, CdSe and CdTe are 21.8 K, 21.2 K and

13.8 K, respectively [37]. However, this value is much larger than that in IV-VI systems with Mn or rare-earth doped.  $|2J/k_B|$  for Mn-doped IV-VI compounds is in the order of 1 K [32]. For example,  $|2J/k_B|$  for Mn-doped PbS, PbSe and PbTe are 2.57 K [38], 3.35 K [32] and 1.69 K [32], respectively. For rare-earth-doped IV-VI compounds,  $|2J/k_B|$  is in the order of 0.1 K [32]. For instance,  $|2J/k_B|$  for  $Pb_{1-x}Eu_xTe$  [39] and  $Pb_{1-x}Gd_xTe$  [32] is 0.23 K and 0.72 K, respectively. This means that the magnitude of nearest-neighbor exchange interaction in  $(La_{1-x}Ba_x)(Zn_{1-x}Mn_x)AsO$  is an order of magnitude higher than that in Mn-doped IV-VI systems, and two orders of magnitude higher than that in rare-earth-doped IV-VI systems.

The magnitude of the nearest-neighbor exchange interaction in  $(La_{1-x}Ba_x)(Zn_{1-x}Mn_x)AsO$  is quite different from that in Mn-doped IV-VI systems; one possible reason is that  $J$  strongly depends on the cation-anion distance in DMSs [32]. CdTe(II-VI DMS), HgTe(II-VI DMS) and PbTe(IV-VI DMS) share almost the same lattice constant  $a$  ( $\sim 6.5$  Å), but their magnitude of exchange interactions are quite different. The cation-anion separation of II-VI systems with zinc-blende or wurtzite structure can be calculated as  $a\sqrt{3}/4$  ( $\sim 2.8$  Å), while the cation-anion separation of IV-VI systems with rock salt structure is  $0.5a$  ( $\sim 3.3$  Å). M. Gorska and J. R. Anderson calculated that this difference in the cation-anion separation alone can lead to an order of magnitude or more difference in the superexchange interaction parameter  $J$  [32], and they believe that superexchange is the dominant exchange mechanism for these DMSs. For LaZnAsO with a ZrCuSiAs-type tetragonal crystal structure, the cation-anion separation of Mn-doped ZnO layer is  $\sim 2.8$  Å, which is close to that in II-VI systems, and explains why the value of  $J$  in  $(La_{1-x}Ba_x)(Zn_{1-x}Mn_x)AsO$  ( $x \leq 0.01$ ) is higher than that in IV-VI systems and close to that in II-VI systems.

We have seen that in, the very dilute regime ( $x \leq 0.01$ ), even carriers and spins are codoped;  $(La_{1-x}Ba_x)(Zn_{1-x}Mn_x)AsO$  do not show any ferromagnetic or spin-glass ordering, similarly to the case of  $La(Zn_{0.9}Mn_{0.1})AsO$  (where no carriers are introduced). This behavior can be explained by models based on random exchange interactions, in which the low-temperature susceptibility follows a power law in temperature as  $T^\alpha$  with  $-1 \leq \alpha \leq 0$  [33]. We plot  $\ln(M-M_0)$  versus  $\ln(T)$  of  $(La_{1-x}Ba_x)(Zn_{1-x}Mn_x)AsO$  for  $0.005 \leq x \leq 0.02$  in Figure 3a. The data can be fitted by straight lines with the slopes as the random-exchange parameters,  $\alpha$ . The plot of  $\alpha$  versus concentration  $x$  is shown in Figure 3b. Note that  $\alpha$  equal to  $-1$  corresponds to a standard Curie-law behavior. For  $x = 0.005$ ,  $\alpha$  is  $-0.91$ , which is quite close to a fully paramagnetic ground state. For  $x = 0.0075$ ,  $\alpha$  ( $\sim -0.98$ ) is closer to  $-1$  than that for  $x = 0.005$ , which is consistent with the magnitude of effective occupation probability of magnetic ion,  $\bar{x}$  ( $\sim 0.0034$  for  $x = 0.0075$ , which is smaller than  $\bar{x} \sim 0.0064$  for  $x = 0.005$ ). As more Ba and Mn are doped, the absolute value of  $\alpha$  is suppressed quickly. For  $x = 0.02$ , the absolute value of  $\alpha$  already decreases to  $\sim -0.3$ , as shown in Figure 3b. The suppression of magnitude of  $|\alpha|$  with increasing  $x$  indicates that increasing carriers and spins concentration enhances the coupling between Mn ions, and eventually results in the formation of ferromagnetic long range ordering.

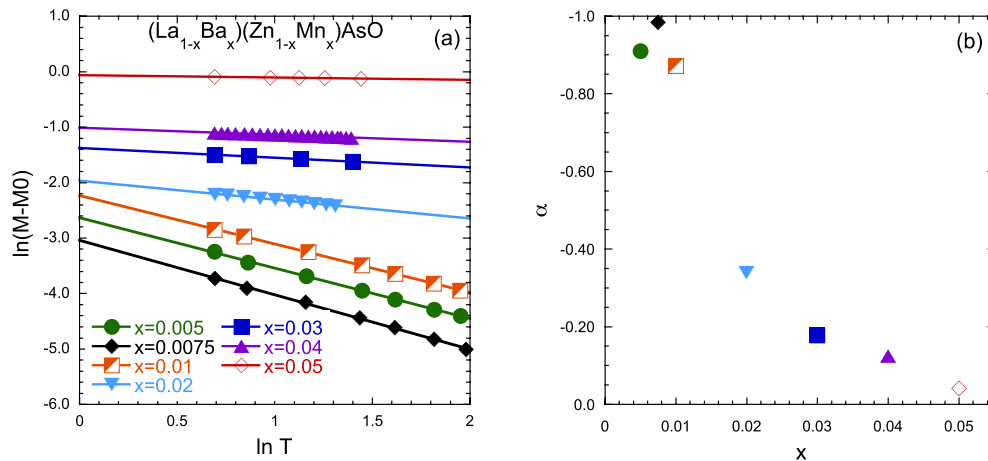


**Figure 3.** (Color online) (a)  $\ln(M - M_0)$  versus  $\ln(T)$  for  $(\text{La}_{1-x}\text{Ba}_x)(\text{Zn}_{1-x}\text{Mn}_x)\text{AsO}$  ( $0.005 \leq x \leq 0.05$ ). Solid lines represent the linear fit. (b)  $\alpha$  obtained in (a) versus the doping concentration  $x$ .

### 3. Materials and Methods

$(\text{La}_{1-x}\text{Ba}_x)(\text{Zn}_{1-x}\text{Mn}_x)\text{AsO}$  polycrystalline specimens were synthesized by solid-state reaction method as described in [21]. High purity elements of La, Zn and As were mixed and heated slowly to 900 °C in evacuated silica tubes, and held for 15 h before shutting off the furnace to produce intermediate products LaAs and ZnAs. LaAs and ZnAs were then mixed with ZnO, BaO<sub>2</sub> and Mn with the stoichiometric composition. The mixture was pressed into pellets and slowly heated up to 1150 °C and kept for 40 h before cooling at a rate of 10 °C/h to room temperature. The polycrystals were characterized via X-ray diffraction at room temperature using a PANalytical X-ray diffractometer (Model EMPYREAN) with monochromatic CuK <sub>$\alpha$ 1</sub> radiation. The dc-magnetization measurements were conducted on a Quantum Design superconducting quantum interference device (SQUID).

### 4. Conclusions

The carrier and spin density of  $(\text{La,Ba})(\text{Zn,Mn})\text{AsO}$  can be accurately controlled with the doping level ranging from 0.005 to 0.05. No ferromagnetic ordering occurs when only doping Mn into the parent compound LaZnAsO up to 10%. With both carriers and moments doping, ferromagnetic ordering starts to form when  $x \geq 0.02$ . With the doping level increasing, the obtained Weiss temperature  $\theta$  changes from negative to positive at  $x = 0.02$ , indicating the dominated exchange coupling between Mn ions is transformed from antiferromagnetic to ferromagnetic. For  $x \leq 0.02$ , the magnetization at low temperature is proportional to  $T^\alpha$  with  $-1 \leq \alpha \leq 0$ , which can be explained by models based on random-exchange interactions. The nearest neighbor exchange interaction parameter  $|2J/k_B|$  is about  $10 \text{ K} \pm 3 \text{ K}$  and  $17 \text{ K} \pm 5 \text{ K}$  for  $x \leq 0.01$  and  $x \geq 0.02$ , respectively. Possessing the advantages of decoupled spin and charge doping,  $(\text{La,A})(\text{Zn,B})\text{PnO}$  ( $A = \text{Ca, Sr, Ba}$ ;  $B = \text{Mn, Fe, Pn} = \text{As, P}$ ) are chemically stable systems for investigation of ferromagnetic mechanism [21–23,25].

**Author Contributions:** Conceptualization, F.L.N.; formal analysis, G.Z. and C.D.; investigation, C.D., K.W., H.Z., S.G., G.Z., Y.G. and L.F.; writing—original draft preparation, C.D.; writing—review and editing, G.Z. and F.L.N.; visualization, C.D. and G.Z.; and supervision, F.L.N.

**Funding:** This research was funded by Key Projects for Research and Development of China (No. 2016FYA0300402), National Natural Science Foundation of China (No.11574265), Natural Science Foundation of Zhejiang Province (No. LR15A040001), and the Fundamental Research Funds for the Central Universities (No. 2017FZA3003).

**Acknowledgments:** F.L. Ning acknowledges helpful discussions with R.N. Bhatt.

**Conflicts of Interest:** The authors declare no conflict of interest. The founding sponsors had no role in the design of the study; in the collection, analyses, or interpretation of data; in the writing of the manuscript, or in the decision to publish the results.



## Abbreviations

The following abbreviations are used in this manuscript:

|          |                                 |
|----------|---------------------------------|
| DMSs     | Diluted Magnetic Semiconductors |
| $\mu$ SR | Muon Spin Relaxation            |
| NMR      | Nuclear Magnetic Resonance      |
| RKKY     | Ruderman–Kittel–Kasuya–Yosida   |
| BMP      | Bound Magnetic Polaron          |
| FC       | Field Cooling                   |
| ZFC      | Zero Field Cooling              |

## References

1. Furdyna, J.K. Diluted magnetic semiconductor. *J. Appl. Phys.* **1988**, *64*, R29.
2. Zutic, I.; Fabian, J.; Das Sarma, S. Spintronics: Fundamentals and applications. *Rev. Mod. Phys.* **2004**, *76*, 323–410.
3. Jungwirth, T.; Sinova, J.; Masek, J.; Kucera, J.; MacDonald, A.H. Theory of ferromagnetic (III,Mn)V semiconductors. *Rev. Mod. Phys.* **2006**, *78*, 809–864.
4. Munekata, H.; Ohno, H.; von Molnar, S.; Segmüller, A.; Chang, L.L.; Esaki, L. Diluted magnetic III-V semiconductors. *Phys. Rev. Lett.* **1989**, *63*, 1849, doi:10.1103/PhysRevLett.63.1849.
5. Ohno, H.; Shen, A.; Matsukura, F.; Oiwa, A.; Endo, A.; Katsumoto, S.; Iye, Y. (Ga,Mn)As: A new diluted magnetic semiconductor based on GaAs. *Appl. Phys. Lett.* **1996**, *69*, 363–365.
6. Samarth, N. A model ferromagnetic semiconductor. *Nat. Mater.* **2010**, *9*, 955–956.
7. Chambers, S. Is it really intrinsic ferromagnetism? *Nat. Mater.* **2010**, *9*, 956–957.
8. Dietl, T. A ten-year perspective on dilute magnetic semiconductors and oxides. *Nat. Mater.* **2010**, *9*, 965–974.
9. Dietl, T.; Ohno, H. Diluted ferromagnetic semiconductors: Physics and spintronic structures. *Rev. Mod. Phys.* **2014**, *86*, 187–251.
10. Dietl, T.; Ohno, H.; Matsukura, F.; Cibert, J.; Ferrand, D. Zener Model Description of Ferromagnetism in Zinc-Blende Magnetic Semiconductors. *Science* **2000**, *287*, 1019–1022.
11. Wang, M.; Champion, R.P.; Rushforth, A.W.; Edmonds, K.W.; Foxon, K.W.; Gallagher, B.L. Achieving high Curie temperature in (Ga,Mn)As. *Appl. Phys. Lett.* **2008**, *93*, 132103.
12. Chen, L.; Yan, S.; Xu, P.F.; Wang, W.Z.; Deng, J.J.; Qian, X.; Ji, Y.; Zhao, J.H. Low-temperature magnetotransport behaviors of heavily Mn-doped (Ga,Mn)As films with high ferromagnetic transition temperature. *Appl. Phys. Lett.* **2009**, *95*, 182505.
13. Chen, L.; Yang, X.; Yang, F.H.; Zhao, J.H.; Misuraca, J.; Xiong, P.; Molnar, S.V. Enhancing the Curie temperature of ferromagnetic semiconductor (Ga,Mn)As to 200 K via nanostructure engineering. *Nano. Lett.* **2011**, *11*, 2584–2589.
14. Deng, Z.; Jin, C.Q.; Liu, Q.Q.; Wang, X.C.; Zhu, J.L.; Feng, S.M.; Chen, L.C.; Yu, R.C.; Arguello, C.; Goko, T.; et al. Li(Zn,Mn)As as a new generation ferromagnet based on a I-II-V semiconductor. *Nat. Commun.* **2011**, *2*, 422–426.
15. Deng, Z.; Zhao, K.; Gu, B.; Han, W.; Zhu, J.L.; Wang, X.C.; Li, X.; Liu, Q.Q.; Yu, R.C.; Goko, T.; et al. Diluted ferromagnetic semiconductor Li(Zn,Mn)P with decoupled charge and spin doping. *Phys. Rev. B* **2013**, *88*, 081203(R).
16. Wang, Q.; Man, H.Y.; Ding, C.; Gong, X.; Guo, S.L.; Wang, H.D.; Chen, B.; Ning, F.L. Li<sub>1.1</sub>(Zn<sub>1-x</sub>Cr<sub>x</sub>)As: Cr doped I-II-V diluted magnetic semiconductors in bulk form. *J. Appl. Phys.* **2014**, *115*, 083917.
17. Ning, F.L.; Man, H.Y.; Gong, X.; Guo, S.L.; Ding, C.; Wang, Q.; Goko, T.; Liu, L.; Frandsen, B.A.; Uemura, Y.J.; et al. Suppression of  $T_c$  by overdoped Li in the diluted ferromagnetic semiconductor Li<sub>1+y</sub>(Zn<sub>1-x</sub>Mn<sub>x</sub>)P: A  $\mu$ SR investigation. *Phys. Rev. B* **2014**, *90*, 085123.
18. Zhao, K.; Deng, Z.; Wang, X.C.; Han, W.; Zhu, J.L.; Li, X.; Liu, Q.Q.; Yu, R.C.; Goko, T.; Frandsen, B.; et al. New diluted ferromagnetic semiconductor with Curie temperature up to 180 K and isostructural to the “122” iron-based superconductors. *Nat. Commun.* **2013**, *4*, 1442–1446.
19. Zhao, K.; Chen, B.J.; Zhao, G.Q.; Yuan, Z.; Liu, Q.Q.; Deng, Z.; Zhu, J.L.; Jin, C.Q. Ferromagnetism at 230 K in (Ba<sub>0.7</sub>K<sub>0.3</sub>)(Zn<sub>0.85</sub>Mn<sub>0.15</sub>)<sub>2</sub>As<sub>2</sub> diluted magnetic semiconductor. *Chin. Sci. Bull.* **2014**, *59*, 2524–2527.

20. Yang, X.J.; Li, Y.K.; Zhang, P.; Luo, Y.K.; Chen, Q.; Feng, C.M.; Cao, C.; Dai, J.H.; Tao, Q.; Cao, G.H.; et al. K and Mn co-doped BaCd<sub>2</sub>As<sub>2</sub>: A hexagonal structured bulk diluted magnetic semiconductor with large magnetoresistance. *J. Appl. Phys.* **2013**, *114*, 223905.
21. Ding, C.; Man, H.Y.; Qin, C.; Lu, J.C.; Sun, Y.L.; Wang, Q.; Yu, B.Q.; Feng, C.M.; Goko, T.; Arguello, C.J.; et al. (La<sub>1-x</sub>Ba<sub>x</sub>)(Zn<sub>1-x</sub>Mn<sub>x</sub>)AsO.: A two-dimensional 1111-type diluted magnetic semiconductor in bulk form. *Phys. Rev. B* **2013**, *88*, 041102(R).
22. Ding, C.; Gong, X.; Man, H.Y.; Zhi, G.X.; Guo, S.L.; Zhao, Y.; Wang, H.D.; Chen, B.; Ning, F.L. The suppression of Curie temperature by Sr doping in diluted ferromagnetic semiconductor (La<sub>1-x</sub>Sr<sub>x</sub>)(Zn<sub>1-y</sub>Mn<sub>y</sub>)AsO. *Eur. Phys. Lett.* **2014**, *107*, 17004.
23. Han, W.; Zhao, K.; Wang, X.C.; Liu, Q.Q.; Ning, F.L.; Deng, Z.; Liu, Y.; Zhu, J.L.; Ding, C.; Man, H.Y.; et al. Diluted ferromagnetic semiconductor (LaCa)(Zn,Mn)SbO isostructural to “1111” type iron pnictide superconductors. *Sci. China-Phys. Mech. Astron.* **2013**, *56*, 2026–2023.
24. Ding, C.; Guo, S.L.; Zhao, Y.; Man, H.Y.; Fu, L.C.; Gu, Y.L.; Wang, Z.Y.; Liu, L.; Frandsen, B.A.; Cheung, S.; et al. The synthesis and characterization of 1111 type diluted ferromagnetic semiconductor (La<sub>1-x</sub>Ca<sub>x</sub>)(Zn<sub>1-x</sub>Mn<sub>x</sub>)AsO. *J. Phys.: Condens. Matter* **2016**, *28*, 026003.
25. Lu, J.C.; Man, H.Y.; Ding, C.; Wang, Q.; Yu, B.Q.; Guo, S.L.; Wang, H.D.; Chen, B.; Han, W.; Jin, C.Q.; et al. The synthesis and characterization of 1111-type diluted magnetic semiconductors (La<sub>1-x</sub>Sr<sub>x</sub>)(Zn<sub>1-x</sub>TM<sub>x</sub>)AsO (TM = Mn, Fe, Co). *Eur. Phys. Lett.* **2013**, *103*, 67011.
26. Yang, X.J.; Li, Y.K.; Shen, C.Y.; Si, B.Q.; Sun, Y.L.; Tao, Q.; Cao, G.H.; Xu, Z.A.; Zhang, F.C. Sr and Mn Co-doped LaCuSO: A wide band gap oxide diluted magnetic semiconductor with T<sub>C</sub> around 200 K. *Appl. Phys. Lett.* **2013**, *103*, 022410.
27. Man, H.Y.; Qin, C.; Ding, C.; Wang, Q.; Gong, X.; Guo, S.L.; Wang, H.D.; Chen, B.; Ning, F.L. (Sr<sub>3</sub>La<sub>2</sub>O<sub>5</sub>)(Zn<sub>1-x</sub>Mn<sub>x</sub>)<sub>2</sub>As<sub>2</sub>: A bulk form diluted magnetic semiconductor isostructural to the “32522” Fe-based superconductors. *Eur. Phys. Lett.* **2014**, *105*, 67004.
28. Guo, S.L.; Ning, F.L. Progress of novel diluted ferromagnetic semiconductors with decoupled spin and charge doping: Counterparts of Fe-based superconductors. *Chin. Phys. B* **2018**, *27*, 097502.
29. Dunsiger, S.R.; Carlo, J.P.; Goko, T.; Nieuwenhuys, G.; Prokscha, T.; Suter, A.; Morenzoni, E.; Chiba, D.; Nishitani, Y.; Tanikawa, T.; et al. Spatially homogeneous ferromagnetism of (Ga,Mn)As. *Nat. Mater.* **2010**, *9*, 299–303.
30. Ding, C.; Qin, C.; Man, H.Y.; Imai, T.; Ning, F.L. NMR investigation of the diluted magnetic semiconductor Li(Zn<sub>1-x</sub>Mn<sub>x</sub>)P (x = 0.1). *Phys. Rev. B* **2013**, *88*, 041108(R).
31. Kusrayev, Y.G.; Kavokin, K.V.; Astakhov, G.V.; Ossau, W.; Molenkamp, L.W. Bound magnetic polarons in the very dilute regime. *Phys. Rev. B* **2008**, *77*, 085205.
32. Gorska, M.; Anderson, J.R. Magnetic susceptibility and exchange in IV-VI compound diluted magnetic semiconductors. *Phys. Rev. B* **1988**, *38*, 9120.
33. Anderson, J.R.; Gorska, M.; Azevedo, L.J.; Venturini, E.L. Magnetization of Hg<sub>1-x</sub>Mn<sub>x</sub>Te. *Phys. Rev. B* **1986**, *33*, 4706.
34. Andres, K.; Bhatt, R.N.; Goalwin, P.; Rice, T.M.; Walstedt, R.E. Low-temperature magnetic susceptibility of Si: P in the nonmetallic region. *Phys. Rev. B* **1981**, *24*, 244.
35. Murayama, C.T.; Clark, W.G.; Sanny, J. Low-temperature magnetic properties of submetallic phosphorous-doped silicon. *Phys. Rev. B* **1984**, *29*, 6063.
36. Bhatt, R.N.; Lee, P.A. Scaling Studies of Highly Disordered Spin-½ Antiferromagnetic Systems. *Phys. Rev. Lett.* **1982**, *48*, 344.
37. Spal/ek, J.; Lewicki, A.; Tarnawski, Z.; Furdyna, J.K.; Galazka, R.R.; Obuszko, Z. Magnetic susceptibility of semimagnetic semiconductors: The high-temperature regime and the role of superexchange. *Phys. Rev. B* **1986**, *33*, 3407.
38. Karczewski, G.; von Ortenberg, M.; Wilamowski, Z.; Dobrowolski, W.; Niewodniczanska-Zawadzka, J. Magnetization of Pb<sub>1-x</sub>Mn<sub>x</sub>S. *Solid State Commun.* **1985**, *55*, 249–252.
39. Braunstein, G.; Dresselhaus, G.; Heremans, J.; Partin, D. Magnetic properties of Pb<sub>1-x</sub>Eu<sub>x</sub>Te grown by molecular-beam epitaxy. *Phys. Rev. B* **1987**, *35*, 1969.





© 2018 by the authors. Licensee MDPI, Basel, Switzerland. This article is an open access article distributed under the terms and conditions of the Creative Commons Attribution (CC BY) license (<http://creativecommons.org/licenses/by/4.0/>).